Geopressured Geothermal Systems: An Efficient and Sustainable Heat Extraction Method

Mauricio A. Rivas, Victoria McGuire, Douglas Simpkins, and Lev Ring

Sage Geosystems

Keywords

Geopressured Geothermal Systems, backpressure, pressure-propped fractures, injection pump parasitic losses, system impedance, no proppant, modeling pressurized systems

ABSTRACT

Conventional geothermal systems rely on production from naturally occurring subsurface hot aquifers, while Hot Dry Rock (HDR) geothermal technology is a method of extracting geothermal energy from deep underground formations where there is hot but dry rock. A downhole heat exchanger is created by water being injected into the rock through one or several wells at high pressure, causing the rock to fracture and creating a network of permeable pathways. Water is then circulated through these artificial or natural fractures, absorbing heat from the hot rock and bringing this heat to the surface.

High impedance in the fracture network and near the wellbore area is a main contributor to high parasitic energy losses in HDR systems and makes commercial-scale implementation very difficult. The Fenton Hill Hot Dry Rock (HDR) tests, from the 1980s and early 1990s, showed that an increased backpressure can reduce markedly the impedance in the system. In so-called doublet (or two-well) Enhanced Geothermal Systems (EGS), horizontal sections of two wells are connected with fractures filled with proppant to prevent these fractures from closing and creating very high resistance to water circulation. This paper provides an alternative solution to the traditional EGS approach and discusses a recently introduced Geopressured Geothermal System (GGS) that keeps the surface and subsurface systems constantly pressurized above fracture opening pressure or, in other words, relying on pressure-propped fractures to keep impedance low.

Focusing on the hydro-mechanical (HM) performance of GGS, and reserving the full thermal-hydro-mechanical (THM) analysis for a later publication, the results show that the single-well pair GGS is superior to other systems in terms of HM performance. The methodology of this single-well pair GGS builds on that of mechanical storage in deep hydraulic fractures as field tested in South Texas in early 2023.

Numerical simulations were performed to demonstrate how properly engineered GGS resolves crucial surface challenges not previously addressed in heat extraction systems and how these geothermal systems experience a lower system impedance while maintaining commercial flow rates. Comparisons are made between GGS with the base case of a doublet EGS whose fractures are proppant-propped. The mathematical modeling of GGS is a natural extension of the recent modeling for mechanical storage that was additionally validated and calibrated against real-time field data.

1. Introduction

Extraction of heat from fractured hot dry rock (HDR) was first proposed in the Los Alamos National Laboratory in New Mexico in the early 1970s (Brown et al. 2012). An early theoretical approach to the heat extraction system studied there comprised two parallel vertical wells drilled to depths reaching dry hot rock with the second well intersecting the vertically oriented fracture produced by hydraulic fracturing the first well (Robinson et al., 1971). However, a more complex HDR system was created from the many years of field development and testing that ensued at Fenton Hill, New Mexico (physical site chosen by Los Alamos; see photo in Figure 1) and which continued until the mid-1990s. A great deal of valuable information was obtained from this pioneering HDR program.

Among the many lessons learned, the Fenton Hill field tests demonstrated that *impedance*, a measure of the resistance to circulation of a fluid through a subsurface system, is greatly reduced by holding an elevated backpressure on the production wellhead which assists in pressure propping the fracture(s) (DuTeau and Brown 1993; see Figure 1 for a recorded table). The potential for electric load-following methods was also verified, but the findings revealed that these backpressure operations: (1) demand a higher injection pumping capacity to maintain a pressurized subsurface system; and (2) expose the surface equipment to higher pressures (Brown and DuTeau 1995).

	LTFT	IFT	IFT2	IFT3
	7/28/92	9/29/92	12/10/92	12/27/92
Injection Pressure, MPa (psi)	27.29 (3958)	22.36 (3243)	27.32 (3963)	27.32 (3962)
Production Pressure, MPa (psi)	9.66 (1401)	9.65 (1399)	15.18 (2201)	12.40 (1798)
Production Flow Rate, l/s (gpm)	5.66 (89.7)	3.85 (61.1)	5.34 (84.6)	5.71 (90.5)
Production Temperature, °C (°F)	183 (361)	165 (329)	177 (351)	183 (361)
*Impedance, MPa/l/s (psi/gpm)	3.11 (28.5)	3.30 (30.2)	2.27 (20.8)	2.61 (23.9)

Figure 1: Photo of the HDR site at Fenton Hill, New Mexico (discover.lanl.gov) and field data demonstrating impedance reduction when applying backpressure via a choke (DuTeau and Brown 1993).

Geopressured Geothermal Systems (GGS), that pressurize the surface and subsurface systems as described in Section 2, are an alternative to previously proposed heat extraction systems as GGS address by design the challenges mentioned above. First, the use of a GGS surface injection kit connected to a high-pressure binary plant allows the use of pressure energy usually wasted at surface to dramatically decrease power lost to the injection pump overcoming impedance; traditional systems simply vent pressures at surface from the production well. Next, fractures are *pressure propped*, defined here as fractures being inflated with fluid pressures above the minimum in-situ stress; the phrase ‘fractures are *operated open’* is also often used. Pressure propped fractures: (a) considerably reduce system impedance, hence reduce friction losses; (b) allow larger lateral well spacing that enable larger fracture areas that are conducive for heat extraction (as opposed to having extensive fractures but short well-to-well distances in each fracture); and (c) enable a single-well pair solution for heat extraction when “huff-n-puff” (cyclical injection-production) operations are implemented instead. Lastly, GGS do not rely on proppants, which induce high friction losses and cannot be uniformly distributed, and thus the associated costs and time of proppant treatments are eliminated.

Because both temperatures and stresses generally increase with depth, a subsurface system reaching practical commercial geothermal temperatures will lead to higher surface pressures if fractures are pressure propped. Hence, the need for a GGS design that can operate with higher pressures both at surface and subsurface. It is noted that operating fracture fluid pressures above the minimum in-situ stress does pose risk to fractures growing. This may lead to fluid being lost as it can be trapped by the fracture at further distances away from the well. More importantly, if fracture growth is uncontrolled, fluid pressurization may trigger seismic activity, particularly if a fault is nearby. Therefore, fluid pressures in opened fractures are further restricted to be below fracture propagation pressures.

Mathematical models have been developed using coupled hydro-mechanical (HM) processes to compare Geopressured Geothermal Systems against a two-well EGS with fractures filled with proppant. A future work will compare the complete thermal-hydro-mechanical (THM) processes of GGS versus EGS. In particular, a future publication will show that the thermal drawdown behavior of a GGS is comparable or better than that of a proppant-laden EGS.

The framework of the engineered systems analyzed in this paper is introduced in Section 2, while Section 3 describes pumping power consumption and system impedance for traditional EGS versus GGS. Completed models are presented in Section 4 and include the deformation and multi-scale nature of fracture propagation; wellbore, perforation, and fracture frictional losses; pressure response due to fluid circulation that includes injection pumping and production; power lost to the injection pump; and system impedance. This section also presents the simulations for all systems and comparisons are made. The final section concludes that the single-well pair GGS, based on cyclic (or huff-n-puff) operations, outperforms any other system.

2. A Proppant-Laden EGS and Three Geopressured Geothermal Systems

The following systems are ordered according to the natural progression from a traditional two-well EGS to the single-well pair GGS design:

I. Two-well system with proppant-laden fractures and continuous circulation of fluid.
II. Two-well system with pressure-propped fractures and continuous circulation of fluid.
III. Three-well system with pressure-propped fractures and continuous circulation of fluid.
IV. Single-well pair system with pressure-propped fractures and huff-n-puff operations.

2.1 Traditional Two-well EGS versus a Two-well GGS.

A two-well Geopressured Geothermal System (GGS) is shown on the right of Figure 2, and this is compared directly with a traditional EGS shown on the left. Both systems have a subsurface design that includes an injection well whose lateral is hydraulically fractured, possibly by employing zonal isolation methods and limited entry completions, and a production well drilled to intersect the multiple fractures created. A first distinct characteristic of the two systems is that the traditional EGS has fractures filled with proppant whereas the GGS does not. In both systems, fluid is circulated down the injector well, through the fracture system and up the producer well.

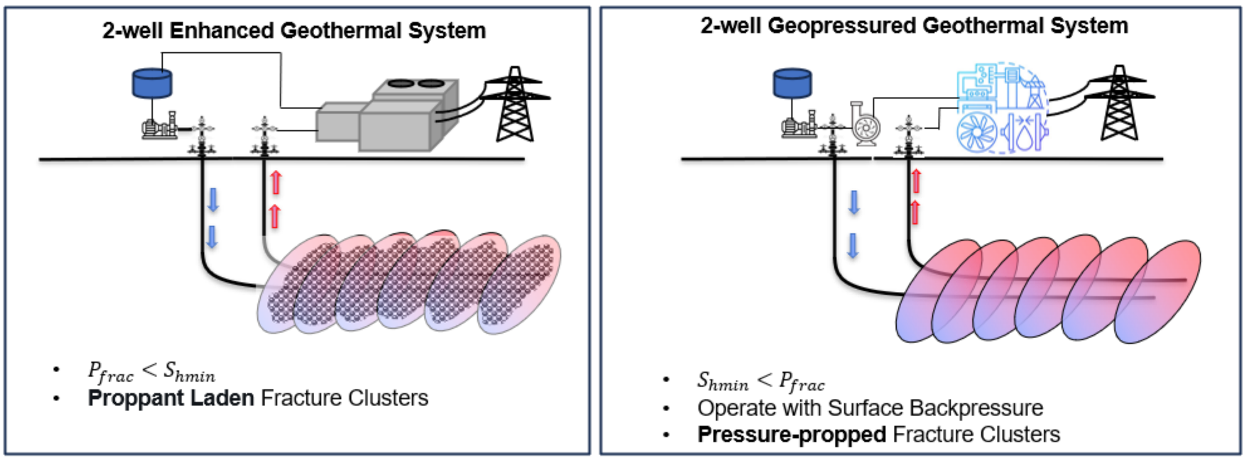

Figure 2: Comparison of a two-well EGS with a two-well GGS.

A second distinction is that the GGS is operated with an elevated backpressure maintained by a controllable choke that connects to the production wellhead. This backpressure is always maintained above fracture opening pressure and thus above the minimum in-situ stress allowing fluid to circulate with minimal impedance.

Although an elevated backpressure reduces the fracture impedance, the injection pump parasitic load increases and this leads to differences in surface design. In a GGS, a high-pressure binary plant (high pressure heat exchanger) maintains the high pressure from the production wellhead side to markedly reduce the pumping power needed by the GGS surface injection side. In this approach, the surface system utilizes pressure energy that is otherwise wasted (vented at surface) in traditional EGS, and allows the subsurface system to be maintained pressurized. A process flow diagram of the surface configuration of the two-well GGS is shown in Figure 3.

This coupling of surface and subsurface leads to a pressurized circulation loop that requires only make-up water to account for losses from evaporation and leak-off to the rock matrix. It should be noted that it is possible for a fracture wing not intersecting a producer well to potentially grow uncontrollably due to the high pressures; this situation is considered in Section 4.

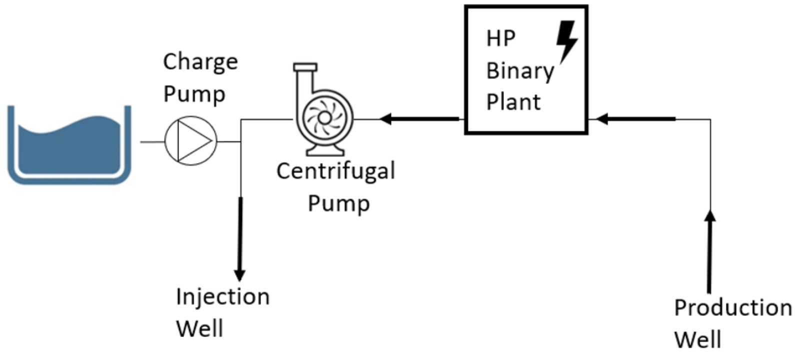

Figure 3: Process Flow Diagram for a two-well GGS; wells are connected at surface by a high-pressure binary plant and a GGS injection surface kit to pressurize the surface system.

2.2 A Pressure-propped Three-well System.

Drilling a second producer well to intersect the fractures of the previous two-well GGS, so that the lateral of the injector well is between both producer laterals, leads to the three-well GGS displayed in Figure 4 (Gedzius et al. 2011). The second producer intersecting the wings previously not containing a producer well reduces the risk of fractures growing out of control.

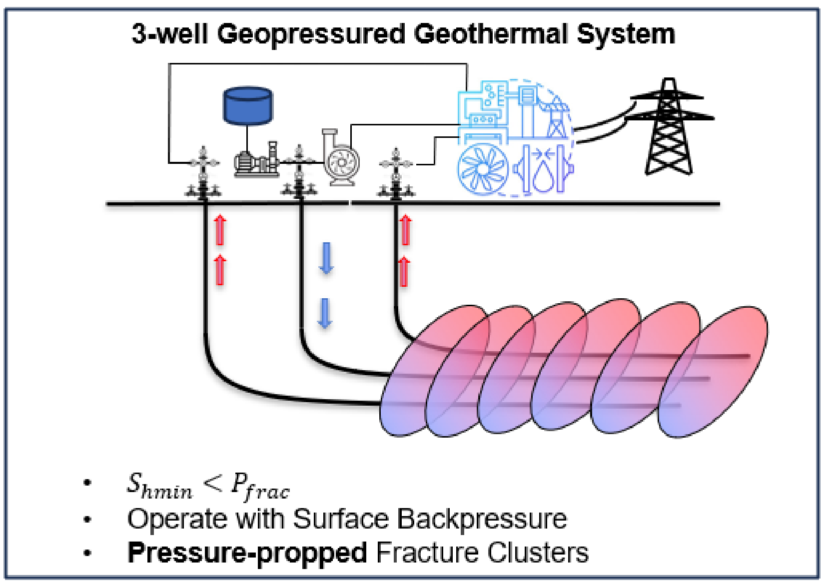

Figure 4: A three-well GGS as an extension of a two-well GGS.

In this design, fluid is circulated down the injector (middle) well, through the fracture cluster, and up through both producer wells. Fractures are opened by the elevated backpressure maintained by controllable chokes at the surface, one on each producer, with fracture fluid pressures maintained above the minimum in-situ stress. The high-pressure heat exchanger in the binary plant uses the high pressures flow from both production wells to significantly reduce the power required by the surface booster injection pump. As in the two-well GGS, this design does not require any proppants to be placed in the fractures.

2.3 A Single-well Pair Geopressured Geothermal System.

A single-well pair GGS operating at two different times is shown in Figure 5 as a 'huff-n-puff' system. In this design wells A and B are not connected in the subsurface and each well has its own set of fractures. This eliminates altogether the expensive task of connecting two or more horizontal wellbores with a fracture system created to establish subsurface circulation. The well stimulation operations are much simpler because each leg can be fracked individually and no intersections are required. The surface system is exactly the same as in other GGS where wells are connected at the surface by a high-pressure binary plant.

The system is initiated by injecting a pre-designed fluid volume and pressurizing fractures in both wells with fluid pressures above the minimum in-situ stress. Fractures in one well are given more fluid than fractures in the other well, and that extra percentage (around 20-30%) of the full fracture fluid volume will be the only volume that is moved back and forth between wells during the cyclic operations. The system is shut-in when the desired pressures and volumes (as calculated to meet power objectives) are reached. The system is now primed and cyclic operations may commence as described next.

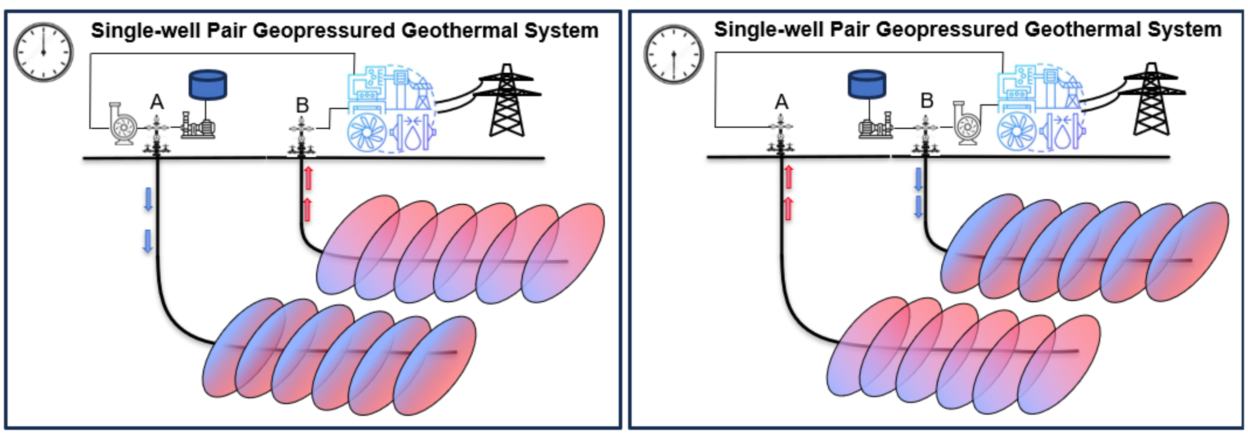

Figure 5: Framework of a single-well pair GGS. Wells are disconnected in the subsurface. Left shows producing from well B and injecting into well A, whereas the right shows producing from A and injecting into B. Surface equipment is not duplicated as flow paths at surface are simply redirected.

Using Figure 5 for illustration, a *cycle* starts at 12 o'clock when well B is opened and the produced fluid is produced to the high-pressure heat exchanger of the binary plant. Then the cooler fluid coming out of this heat exchanger is injected into well A while maintaining high pressure. As mentioned above, only a percentage of the total fluid volume is moved from well B fractures to well A fractures. The extra percentage of (cooler) fluid injected into well A fractures mixes with the volume of fluid injected during the initiation phase that is by now additionally heated. This percentage is calculated so that the system, in the example of Figure 5, runs until 6 o'clock, at which time well A fractures have the bigger fracture fluid volume. Now the wells are shut-in and then flow is reversed to begin the second half of the cycle, as in the right side of Figure 5. It is also possible to have a shut-in period before reversing the flow but this depends on power objectives. In this second half of the cycle, well A produces hot (due to mixing) pressurized fluid into the high-pressure binary plant and the same surface injection kit now injects the cooler fluid into well B. This A-to-B flow runs until 12 o'clock, the time when a full cycle is complete and well B fractures again have a larger volume than well A fractures. The wells are shut-in at 12 o'clock to then reverse the flow and start the second cycle. Running consecutive cycles creates the cyclic (or huff-n-puff) operations of this single-well pair GGS.

3. Minimizing the Power Lost to the Injection Pump and Impedance

The pressurized surface system in a general GGS arises from the need to decrease pump power consumption for the overall system to be practical. Since the power consumed by a pump is given by

$$Power_{pump} = \frac{(P_{pump} - P_{suction})\dot{m}_{inj}}{\rho_{inj}\eta_{pump}}, \quad (1)$$

where $(P_{pump} - P_{suction})$ is the pressure differential across the pump, $\dot{m}_{inj}$ is the mass flowrate at the injector well, ρ_{inj} the density of the fluid and η_{pump} is the efficiency of the injection pump, power is minimized by minimizing the pressure differential across the pump. An innovative solution to reduce the power consumed by the pump is to maintain the backpressure through the whole surface system. This leads to two types of surface systems where one operates with a low suction pressure (LSP) pump and the other with a high suction pressure (HSP) pump. In the simulations presented here, the efficiencies for the pumps are assumed to be 0.7 and 0.85, respectively, for the HSP and LSP pumps.

Figure 6 shows hydraulic schematics for two surface/subsurface systems where the subsurface system is either connected by fractures (left) or disconnected (right). The pump in either schematic may be LSP or HSP.

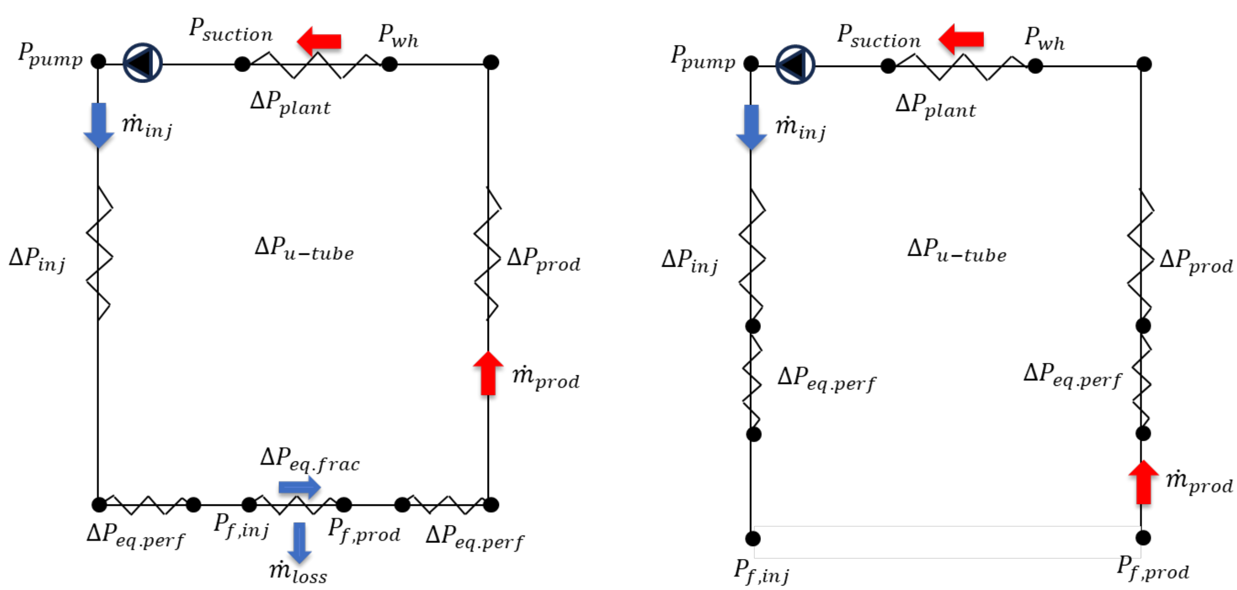

Figure 6: Hydraulic schematics of the surface/subsurface system comprising two vertical wells connected by fractures (left) and disconnected in the subsurface (right).

Using the hydraulic schematic on the left in Figure 6, the pressure balance for a system that circulates fluid is given by

$$P_{pump} - P_{suction} = \Delta P_{plant} + \Delta P_{wells} + \Delta P_{eq.perfs} + \Delta P_{eq.frac} + \Delta P_{u-tube} \quad (2)$$

where $P_{suction}$ is the suction pressure, ΔP_{wells} combines the injection and production well pressure losses denoted by ΔP_{inj} and ΔP_{prod}, respectively, $\Delta P_{eq.perfs}$ is pressure loss due to perforations, $\Delta P_{eq.frac}$ is fracture pressure loss, and ΔP_{u-tube} is the hydrostatic differential pressure between wells. The *system impedance* that the pump needs to overcome is

$$\text{Impedance} = \left(P_{pump} - P_{suction} - \Delta P_{u-tube}\right)/Q_{prod} \tag{3}$$

where Q_{prod} is the volumetric flowrate at the production side.

When wells are disconnected at subsurface (right side of Figure 6), both formulas are the same except that the fracture pressure difference $\Delta P_{eq.frac}$, between $P_{f,inj}$ and $P_{f,prod}$, refers to fracture fluid pressures in the same fracture (when circulating fluid between wells in the subsurface) or pressures in disconnected fractures (when cycling fluid between wellbores to surface, without subsurface connection). When more than one fracture or producer well is involved, then the schematics of Figure 6 extend, and so do the formulas, in a similar fashion as in parallel circuit analysis.

4. Modeling and Results for Pump Power Consumption and Impedance

Simulations for the GGS designs while in operation were made here with a hydro-mechanical (HM) solver. Fractures are assumed to be height constrained and below an effective stress and pressure sealing formation to prevent upward growth. The deformation and near-tip behavior of propagating fractures governed by competing processes is captured by the solver by modeling fractures as one-dimensional objects embedded in a two-dimensional reservoir. Fluid balances, leak-off, and fracture contact are also handled. The simulator includes wellbores connected to fractures with perforations and simulates the pressure response due to either circulating fluid through the entire subsurface system or cycling fluid between two disconnected well/fracs system. For the surface system, the simulator also calculates power lost to the injection pump and system impedance.

The wells for each of the modeled cases reach a true vertical depth of 7500 ft (2286 m), and laterals 3281 ft (1000 m) long connect with 100 fractures for all cases except the single-well pair GGS that only has 8 fractures on each of its 262 ft (80 m) long laterals; 7” casing for the entire lengths of the wells is assumed for each well; when wells are connected by fractures the spacing between laterals is set to be 656 ft (200 m). Pore pressure is taken to be hydrostatic and a gradient of 0.7 psi/ft is assumed for the minimum horizontal stress, with a normal fault regime. The reservoir rock at the given depth is assumed to have a permeability of 0.1 mD, a Young’s modulus of 20 GPa, and a Poisson’s ratio of 0.25.

The fluid in each of the systems is assumed to be water, and though temperature is not explicitly modeled, it is prescribed at 40 °C for injection wells and 150 °C for the reservoir/fractures and production wells. As fluid properties depend on pressure and temperature, thermophysical properties of the fluid are obtained by the equation of state using REFPROP (Lemmon et al. 2018).

All of the above also holds for the traditional two-well EGS, except that fractures are modeled differently. They are treated to be in the ideal case where each fracture is filled with uniformly distributed proppant so that a 0.5 porosity, a fracture conductivity of 25 md-ft, and a 1.5 mm aperture is assumed for each fracture.

4.1 Impedance and Pump Power Consumption in a Traditional Two-well EGS

A traditional two-well EGS, as in the left of Figure 2 but with 100 fractures, is modeled here under the assumptions given above. In the following, the simulator has filled the fracture/well system to initiate modeling of the system in full operation.

Figure 7 shows the simulated behavior of this two-well EGS operating for two days. A constant 50 l/s (793 gpm) injection flowrate is specified for the entire modeled time, while the backpressure is controlled to stepwise increase from a constant 100 psi (0.69 MPa) on the first day to a constant 200 psi (1.38 MPa) on the second day.

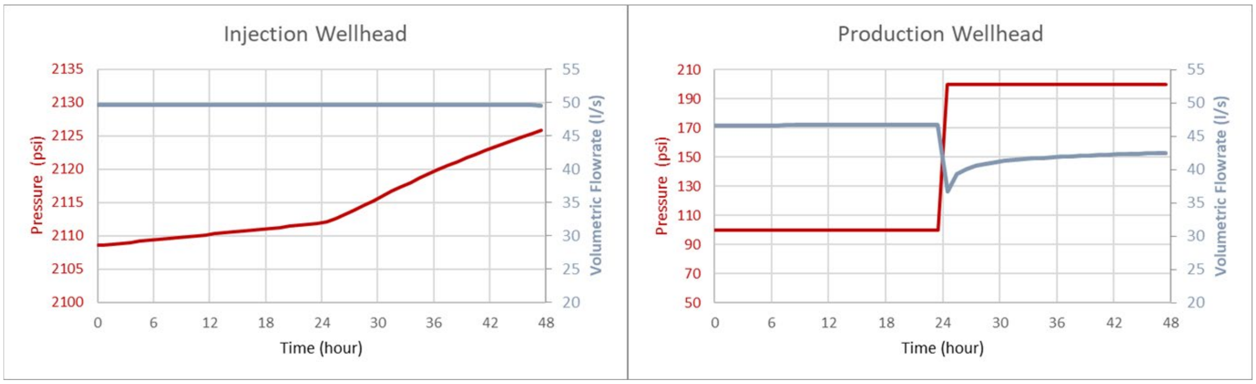

Figure 7: Simulated behavior of a traditional two-well EGS with 100 proppant-laden fractures operated with constant backpressures on each of the two days.

The simulation shows that on both days the production flowrate remains near constant, with approximately 47 l/s (745 gpm) on the first day and then drops and rebounds to the lower value of about 42 l/s (666 gpm) on the second day when the production backpressure is stepwise increased. The injection wellhead pressure builds up approximately linearly on both days, but at a much faster rate on the second day in response to the increased backpressure.

Figure 8 provides the friction pressure losses experienced during these two days of operation that circulates fluid down the injector well, through the 100 proppant-laden fractures and up the producer well; the part that makes up the U-tube effect is shown in the secondary vertical axis.

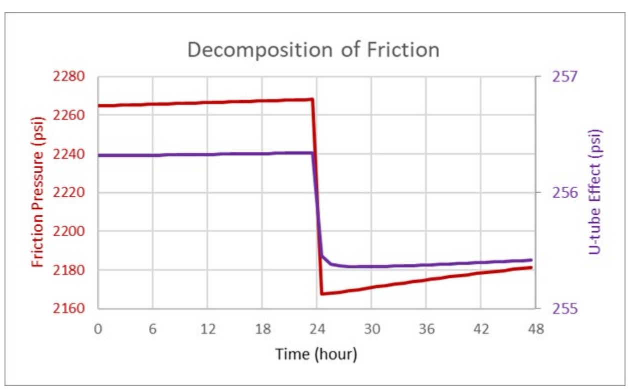

Figure 8: Friction pressure and U-tube effect of the two-well EGS with 100 proppant-laden fractures.

During the first day, the friction pressure remains around 2265 psi (15.62 MPa), and drops to 2167 psi (14.94 MPa) on the second day after the backpressure stepwise increases. This friction pressure increases just slightly on the first day and moderately on the second day. It is observed that the U-tube effect follows a similar trend, but with magnitudes equal to 256 psi (1.77 MPa), on average, throughout the two-day operation.

Now the system impedance and pump consumption of power, are displayed in Figure 9. When the surface system is pressurized and an HSP pump used, then the system impedance on the first day is observed to be 0.35 MPa/(l/s) and increases and rebounds to 0.37 MPa/(l/s) on the second day as a consequence of the added resistance when the production backpressure is increased. When the surface system is not connected and an LSP pump is used, the impedance is 0.36 MPa/(l/s) on the first day and 0.40 MPa/(l/s) on the second day. This gives only a 3-8% drop in impedance when pressurizing the surface system.

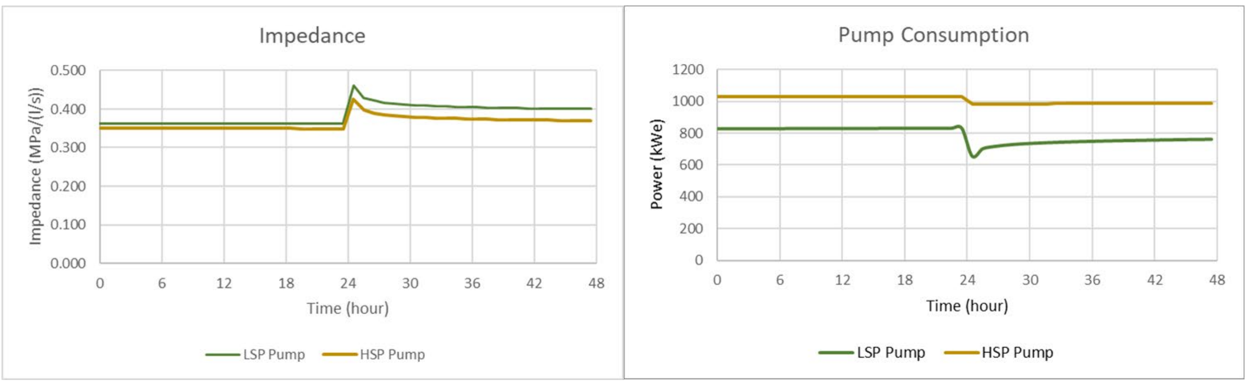

Figure 9: System impedance and pump power consumption for a traditional two-well EGS with 100 proppant-laden fractures.

When the EGS is operated with an LSP pump, the power consumed by the pump is 830 kWe, on average, during the first day of operation, and this drops but gradually increases to 762 kWe during the next 24 hours to overcome the stepwise increased backpressure. If, however, this two-well system is pressurized at surface and an HSP pump is used, then the pump consumption is about 1031 kWe during the first day and drops to 983 kWe and gradually increases to 990 kWe during the second day.

Modeling thus shows that maintaining the surface pressurized in a system where fractures are proppant propped leads to higher impedance and a power consumption increase of about 201 kWe during the first 24 hours and about 228 kWe during the next 24 hours. This translates to an energy increase of 4,824 kWh on the first day and 5,472 kWh on the second. Therefore, pressurizing the surface system when propping the fracture system with proppant is undesirable.

4.2 Reducing Impedance and Pump Power Consumption in a Two-well GGS

This subsection shows that hastily pressure propping fractures and pressurizing the surface system of a doublet system may be unwise and that careful attention is needed for a properly engineered GGS. Here, a two-well system is considered, as in the right of Figure 2 but with 100 fractures that are pressure-propped as opposed to proppant-propped. Since the fractures are operated open, i.e. with fluid pressures above the minimum in-situ stress, the deformation part of the simulator is enabled. In the following, the simulator has filled and pressurized the fracture/well system to initiate modeling of the system in full operation. Fractures fluid pressures are above the minimum in-situ stress but below the pressure that would lead to fracture propagation.

Figure 10 shows the simulated behavior of this two-well GGS operating for two days. A constant 50 l/s (793 gpm) injection flowrate is specified while maintaining a constant backpressure of 2132 psi (14.7 MPa) for the entire simulation.

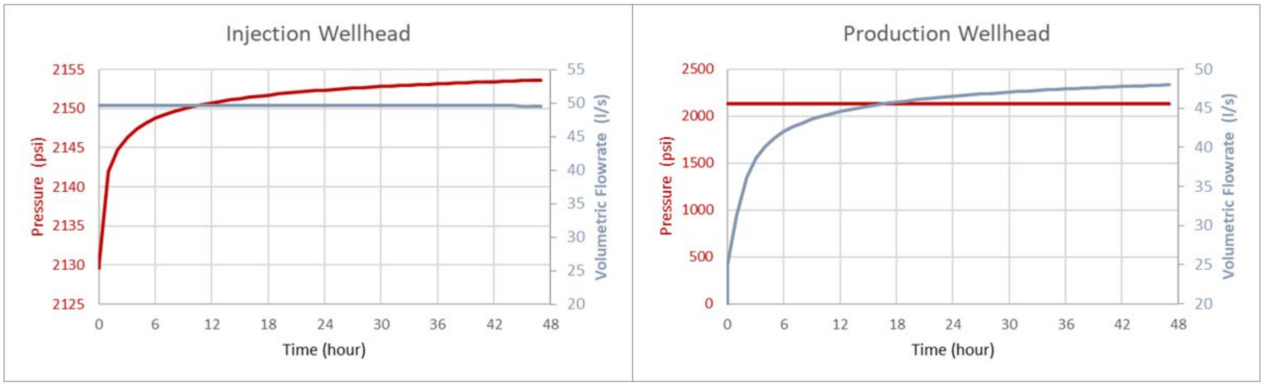

Figure 10: Simulated behavior of a two-well GGS with 100 fractures operated with a constant backpressure during the entirety of two days.

The simulation shows that the production flowrate increases from 25 l/s (396 gpm) to reach 48 l/s (761 gpm) at the 48th hour of operation as the increasing rate slows down. It is seen that the injection wellhead pressure builds up sharply during the initial 4 hours and continues to increase afterwards but at a much slower rate.

The friction pressure losses experienced by this pressurized system during these two days of operation is shown in Figure 11; the part that makes up the U-tube effect is again separated into the secondary vertical axis. The friction pressure is about 254 psi (1.75 MPa) for the 23 hours after having sharply increased in the first hour from the initial 156 psi (1.08 MPa). This friction pressure increases very slowly in the last 23 hours of operation. The U-tube effect is close to 233 psi (1.61 MPa) during the modeled time.

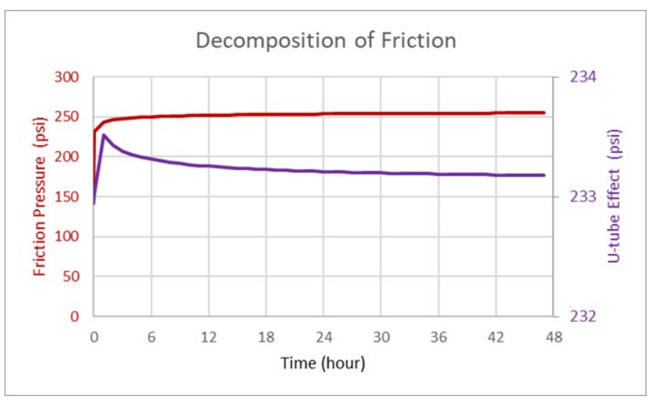

Figure 11: Friction pressure and U-tube effect of the two-well GGS with 100 fractures.

Figure 12 displays the system impedance and pump consumption of power. If the surface system is pressurized and uses an HSP pump, the system impedance is around 0.053 MPa/(l/s) for the majority of the two days, though it is gradually decreasing. If the surface is not pressurized and is equipped with an LSP pump, then the impedance is about 0.36 MPa/(l/s) throughout the modeled time. The impedance of the fully pressurized system is about an order of magnitude less than when the surface is not pressurized; this is also true when comparing with the proppant-laden EGS case.

Moreover, the maximum fracture aperture observed was 0.8 mm when fractures are pressured propped, almost half the aperture size of the proppant propped factures.

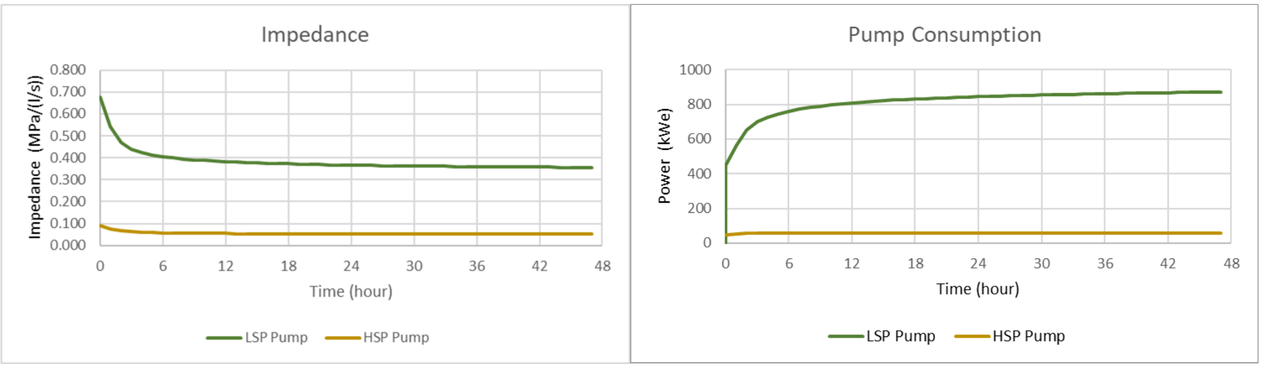

Figure 12: System impedance and pump power consumption for the two-well GGS.

Consider now the pump consumption behavior for this two-well system. Suppose first that this system is operated with an LSP pump. Figure 12 shows that the power consumed by the pump is 798 kWe, on average, during the two days of running the system. If, however, the surface system is pressurized and equipped with an HSP pump, then the pump consumption drops to 58 kWe during the modeled time. Thus, maintaining the surface system pressurized drastically reduced the power consumption of the pump. In fact, the drop in power consumed by the pumps implies an energy drop of 35,520 kWh during these two days.

The reduced impedance, the energy difference and the favorable system performance observed seems to undoubtedly warrant the use of a GGS surface injection kit for a two-well system. However, the simulations reveal a serious issue. Figure 13 shows a plan view of reservoir pressure focusing on one fracture in the system, and where the injector/producer well pair (two points) roughly are, respectively, at the centers of the red/blue region in the first frame, with this well distance fixed in all four frames. The simulation shows that the fracture keeps growing to the right, whereas the producer well serves as a pressure barrier and obstructs fracture growth to the left. Continued fracture growth is unwanted when continuously operating any heat extraction system as fluid is lost in the 'opposite direction'. More importantly, in scenarios of low fracture toughness, as in the simulation, the risk of uncontrolled fracture propagation is possible and may lead to seismic activity. As this may not always happen, operating a two-well system with fractures pressure propped and with a pressurized surface should be done with great caution if not avoided.

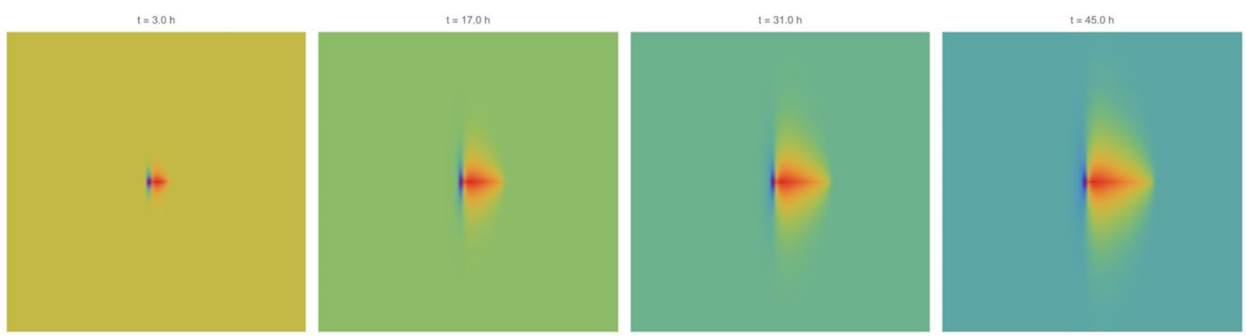

Figure 13: Plan view of reservoir pressure at hour 3, 17, 31 and 45 of the simulation displaying one fracture continuously growing to the right.

These modeled results align with the observations at Fenton Hill where the field tests of the (much more complex) subsurface system subjected to high injection and production pressures showed micro-seismic activity that implied further reservoir growth (Brown 1994). The recommendation from the Los Alamos National Laboratory to include a secondary production well, opposite the first relative to the injector well, is simulated next.

4.3 Reducing Impedance and Pump Power Consumption in a Three-well GGS

This subsection models operating a three-well GGS as in Figure 4 but with 100 fractures. As in the two-well GGS, fracture deformation is fully accounted for by the simulator. To initiate modeling of the system in full operation, the simulator fills the subsurface system and pressurizes the fractures with fluid pressures above the minimum in-situ stress but below the threshold that would lead to fracture propagation.

Figure 14 shows the simulated behavior of this three-well GGS operating for 48 hours. A constant injection flowrate of 50 l/s (793 gpm) is again specified for the entire modeled time, but the backpressure is controlled, in this case, to decrease stepwise from a constant 2132 psi (14.7 MPa) on the first day to a constant 2103 psi (14.5 MPa) on the second day.

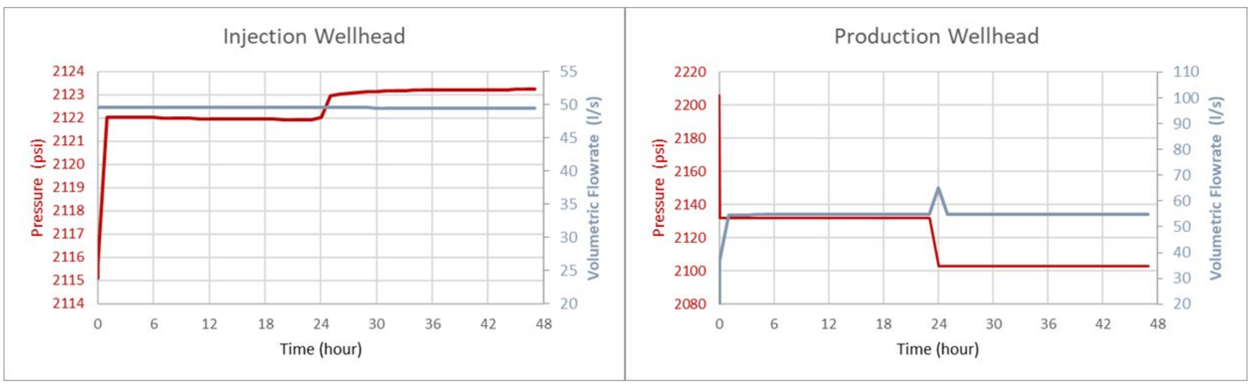

Figure 14: Simulated behavior of a three-well GGS with 100 fractures with fluid pressures above the minimum in-situ stress but below fracture propagation.

On both days the production flowrate remains a near constant of 55 l/s (872 gpm), with a small spike around the 24th hour when the backpressure is stepwise reduced. The injection pressure (approximately) stepwise increases from 2122 psi (14.63 MPa) on day one and to 2123 (14.64 MPa) on day two in response to the decreased backpressure in this system where fractures are operated open.

Figure 15 displays the friction pressure losses experienced during these two simulated days of injection and production; the part that makes up the U-tube effect is again on the secondary vertical axis. Compared with results for the EGS recorded in Figure 11, the friction pressure in this three-well GGS is lower by one order of magnitude. While operating this three-well system, the friction pressure loss is 223 psi (1.54 MPa) on the first day, and increases to 254 psi (1.75 MPa) on the second day after the backpressure stepwise decreases. The U-tube effect follows a similar stepwise increasing behavior, but is on average about 233.5 psi (1.61 MPa). Note that this U-tube effect, and that of the two-well GGS case, are close to the 256-psi average U-tube effect for the proppant-laden two-well EGS.

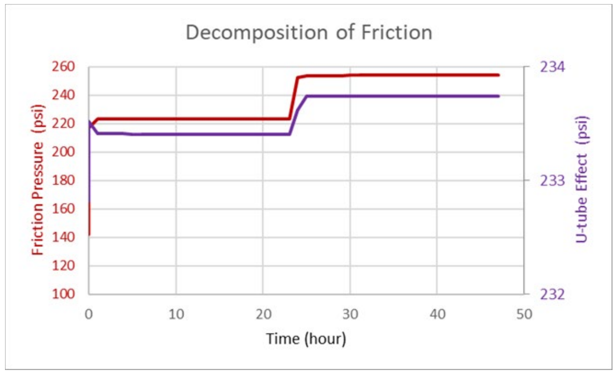

Figure 15: Friction pressure and U-tube effect of the three-well GGS with 100 fractures.

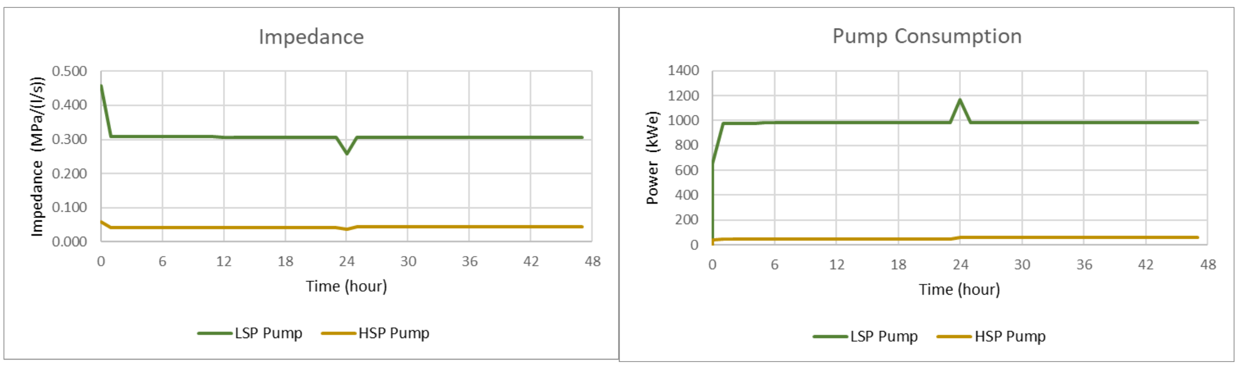

Figure 16: System Impedance and Pump Power Consumption for a three-well GGS with 100 fractures.

When the surface is pressurized and an HSP pump is used, Figure 16 shows that the system impedance is 0.041 MPa/(l/s) on the first day and increases to 0.044 MPa/(l/s) on the second day when the backpressure is stepwise decreased. When the surface is not connected and an LSP pump is used, the system impedance is 0.307 for the majority of the simulated time. As with friction pressure, the impedance of this pressurized system is an order of magnitude less than the unpressurized surface case; this observation is also true when comparing with the proppant-laden EGS case. The maximum fracture aperture observed when fractures were pressure propped was 0.95 mm, 37% less than the fracture aperture in the EGS case.

If the three-well subsurface system is operated with an LSP pump, the power consumed by the pump is 958 kWe during the two days simulated operation. However, if the surface system is pressurized and an HSP pump used, then the pump consumption stepwise increases from 43 to 58 kWe from day one to day two. This (small) jump results since the production backpressure is lower on the second day.

The simulations thus show that pressurizing the surface system leads to a power consumption drop of 907 kWe, on average, during the two-day operation. This translates to an energy drop of 43,536 kWh during this two-day simulation.

4.4 Reducing Impedance and Pump Power Consumption in a Single-well Pair GGS

This last design, the single-well pair GGS as in Figure 5 but with 8 fractures, is operated with cyclic, or huff-n-puff, operations, so the modeling results are displayed in a slightly different manner. As in the previous GGS designs modeled, fracture deformation is fully accounted for by the simulator as fractures are pressure-propped. To initiate modeling of the system in full operation, the simulator fills and pressurizes the fractures on both wells with fluid pressures above the minimum in-situ stress but below the pressure that would yield fracture propagation.

Figure 17 shows the simulated behavior of this single-well pair GGS operating for 52 hours. Consider first the flowrate profile of well A (in black). For the first 5.5 hours, fluid is being produced by well A at a rate of 50 l/s (793 gpm) and injected into well B; this is indicated in the plot by the negative volumetric flowrate value for well A. This production phase is followed by a one-hour shut-in phase of well A, and subsequently a 5.5-hour phase of injecting fluid (from well B) into well A at a rate of 50 l/s (a positive value in the plot). Another shut-in phase for one hour of well A follows, and then this production-injection process is repeated for well A. This creates the cyclic operation of well A, and well B is operated similarly but with the flow opposite that of well A. The accompanying plot shows that wellhead A pressure, for example, decreases when well A is producing, rebounds when shut-in, and increases when injecting into well A. Well B follows the same wellhead pressure behavior.

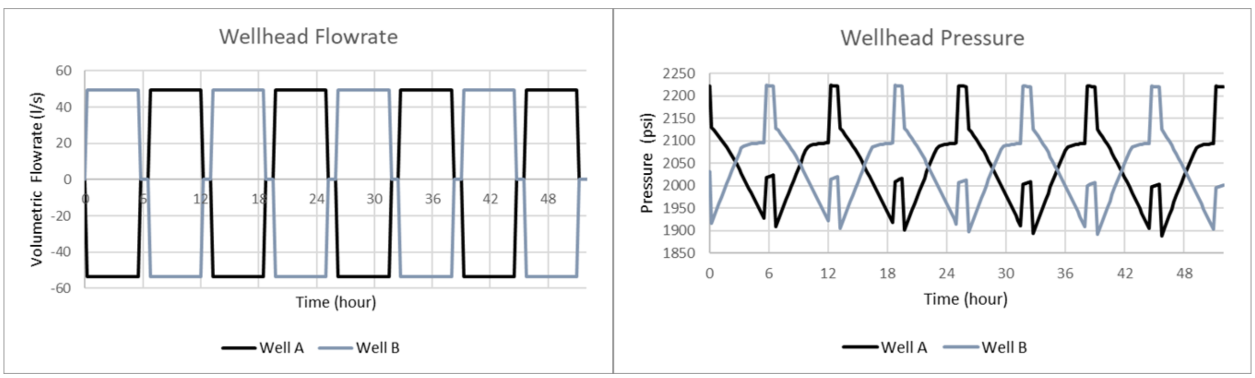

Figure 17: Simulated behavior of a single-well pair GGS with 8 fractures per well and huff-n-puff operations.

Figure 18 displays the friction pressure losses experienced during these 52 hours of huff-n-puff operations; the part that makes up the U-tube effect is shown in purple.

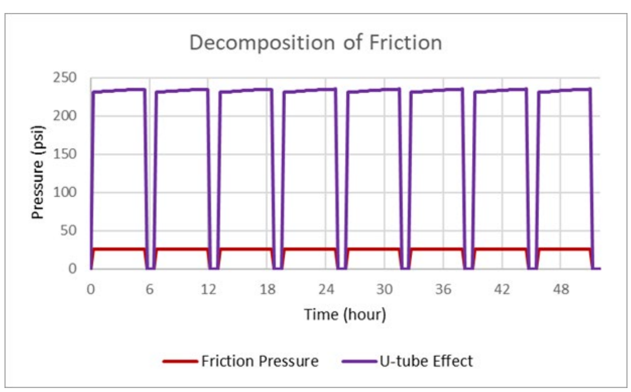

Figure 18: Friction pressure and U-tube effect of the single-well pair GGS with 8 fractures per well.

Unlike the other GGS designs, the friction pressure losses for the single-well pair GGS are one orders of magnitude lower than that experienced in the EGS with proppant-laden fractures; this single-well pair GGS has a friction pressure loss of 26 psi (0.18 MPa). The U-tube effect for the single-well pair GGS is 233 psi (1.61 MPa) when flowing, similar to the previous two GGS designs.

From Figure 19, the system impedance for the single-well pair design with the surface system pressurized (and thus with an HSP pump) has a value of 0.16 MPa/(l/s) when flowing. If the wells are not connected at surface and an LSP pump is used, then the system impedance is 1.16 MPa/(l/s), which is almost an order of magnitude higher than with the HSP pump. The maximum aperture observed for this case was 0.7 mm, which is less than half the aperture size in the EGS case.

If this two-well system is operated with an LSP pump, then the power consumed by the pump is 856 kWe, on average, during the simulated transfer of fluid. However, if the surface system is pressurized and an HSP pump is used, then the pump consumption is 80 kWe, on average, when flowing.

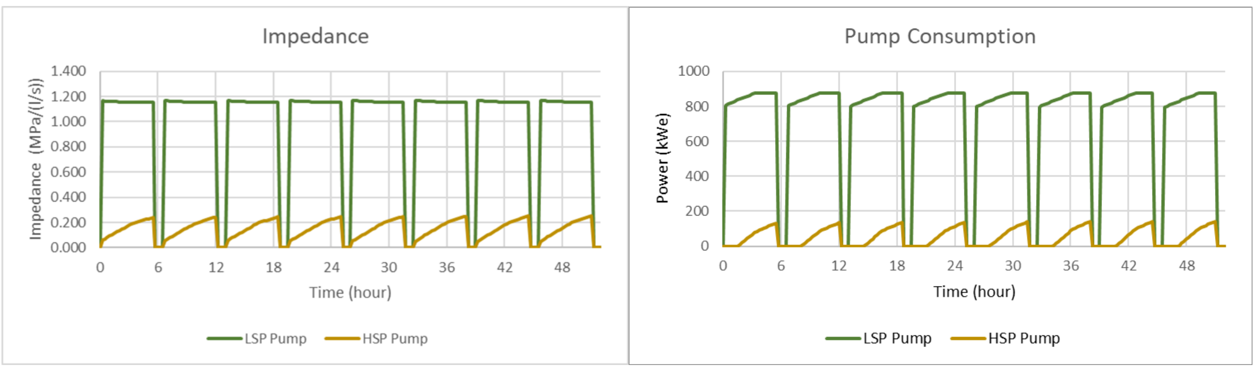

Figure 19: System Impedance and Pump Power Consumption for a single-well pair GGS.

Results from the simulation thus shows that maintaining the surface system pressurized leads to a power consumption drop of about 776 kWe during the 5.5 hours of flow. This translates to an energy drop of 4,265 kWh (on average) for each of these 5.5 hours of fluid transfer, or 34,144 kWh in the time when flowing.

5. Summary and Conclusion

These simulation results show that subsurface systems with pressure propped fractures have an impedance about one order of magnitude lower when the surface system is pressurized and when using a High Suction Pressure (HSP) pump versus not pressurizing the surface and only using a Low Suction Pressure (LSP) pump. This holds regardless if fluid is circulated through a connected subsurface or if huff-n-puff operations are used between two wells disconnected at the subsurface. The two-well and three-well designs where the surface and subsurface systems are pressurized have an impedance one order of magnitude lower than in the traditional two-well EGS with proppant propped fractures and an LSP pump. The pressurized single-well pair design with wells disconnected at the subsurface, but connected and pressurized at the surface, has half the impedance experienced in the EGS case.

If the surface system is pressurized and an HSP pump used when operating fractures open, then the power consumed by the injection pump is only 6-9% of the power consumed if an LSP pump is utilized (and if the surface system is not pressurized). In other words, maintaining the whole system pressurized, instead of wasting pressure on the production side, allows to drastically cut injection pump parasitic costs.

However, care should be taken when pressurizing the entire system. When applying this methodology to a two-well, multi-fracture system, the simulations show that continuous operation of the system (with practical performance at surface) leads to continued fracture growth, hence major fluid losses. Therefore, a GGS design should be operated with fracture fluid pressures above the minimum horizontal stress and below that which would induce fracture propagation. Both the three-well and single-well pressurized systems successfully use this pressure window. Longer lateral spacing is also demonstrated by the three-well design. The pressurized single-well pair design based on huff-n-puff operations is seen to be superior to the other systems in terms of the hydro-mechanical performance and it simplifies the stimulation operations and reduces the number of fractures by an order of magnitude.

Complementing the presented analysis of the GGS approach, a next publication will treat the full thermo-hydro-mechanical performance of GGS design.

Acknowledgement

Special thanks to our CTO Lance Cook at Sage Geosystems for the insightful subsurface design guidance.

REFERENCES

Brown, D. "How to Achieve a Four-fold Productivity Increase at Fenton Hill." *GRC Transactions,* Vol. 18 (1994).

Brown, D., Duchane, D.V., Heiken, G. and Hriscu, V.T. "Mining the Earth's Heat: Hot Dry Rock Geothermal Energy." *Springer-Verlag,* Berlin Heidelberg (2012).

Dontsov, E.V., and Peirce, A.P. "A multiscale Implicit Level Set Algorithm (ILSA) to model hydraulic fracture propagation incorporating combined viscous, toughness, and leak-off asymptotics." Comput. Methods Appl. Mech. Engrg. 313 (2017).

DuTeau, R. and Brown, D. "HDR Reservoir Flow Impedance and Potentials for Impedance Reduction." *Proceedings: 18th Workshop on Geothermal Reservoir Engineering*, Stanford University, Stanford, CA (1993).

Gedzius I, Teodoriu C. "Innovative Erschliesungskonzepte für Hot-Dry-Rock-Projekte im Norddeutschen Becken." DGMK/€OGEW-Frühjahrstagung. Fachbereich Ausführung und Gewinnung (2011).

Glauser, W., McLenna, J. and Walton, I. "Do Perforated Completions have value for Engineered Geothermal Systems." *ISRM International Conference for Effective and Sustainable Hydraulic Fracturing,* Brisbane, Australia (2013).

Lemmon, E.W., Bell, I.H., Huber, M.L., McLinden, M.O. "NIST Standard Reference Database 23: Reference Fluid Thermodynamic and Transport Properties-REFPROP." Version 10.0, National Institute of Standards and Technology, Standard Reference Data Program, Gaithersburg (2018).

Murphy, H.D., Tester, J.W., Grigsby, C.O. and Potter, R.M. "Energy Extraction from Fractured Geothermal Reservoirs in Low-Permeability Crystalline Rock." *Journal of Geophysical Research*, Vol. 86, No. B8, pp. 7145-7158 (1981).

Robinson, E.S., Potter, R.M., McInteer, B.B., Rowley, J.C., Armstrong, D.E., Mills, R.L. and Smith, M.C. "A preliminary study of the nuclear subterrane." *Los Alamos Scientific Report,* Rept. LA-4547 (1971).

Simpkins, D., Rivas, M.A., Eros, M. and Ring, L. "Energy Storage in Deep Hydraulic Fractures: Mathematical Model and Field Validation." *GRC Transactions*, Vol. 47 (2023).